



Friedrich-Alexander-Universität  
Faculty of Engineering

Department Materials Science

WW8: Materials Simulation

## **Practical: Phase-Field Method**

Basics and Application in Materials Science

Leon Pyka (22030137)

**Supervision: Dr. Frank Wendler**

## Contents

1	Introduction	2
2	Task 1: 1D Single-Component Solidification	2
3	Task 2: Determination of $f_0$	5
4	Task 3: Determination of $K_c$	8

## 1 Introduction

Phase-field simulation is a versatile application in the toolbox of materials simulation. It is often used for simulations of phase transitions, dislocation evolution, fracture simulations etc. The following practicals aim is to get a practical introduction into the subject. In two separate tasks a 1D single-component solidification simulation, calculation of a bulk energy density coefficient and gradient energy density coefficient are going to be conducted.

## 2 Task 1: 1D Single-Component Solidification

To simulate a 1D single-component solidification we utilize the following energy density:

$$F = \int (f_0 \phi^2 (1 - \phi)^2 + \frac{K_\phi}{2} |\nabla \phi|^2) d\vec{r} \quad (1)$$

As solidification is a non-conservative process, the kinetics are governed by the Allen-Cahn equation (for the homogeneous, isotropic case).

$$\frac{\partial \phi}{\partial t} = -L \frac{\delta F}{\delta \phi} \quad (2)$$

Here the functional derivative  $\frac{\delta F}{\delta \phi}$  of an energy functional eq. 3a can be evaluated as eq. 3b.

$$F = \int f(\vec{r}, \phi, \nabla \phi) d\vec{r} \quad (3a)$$

$$\frac{\delta F}{\delta \phi} = \frac{\partial f}{\partial \phi} - \nabla \cdot \frac{\partial f}{\partial (\nabla \phi)} \quad (3b)$$

Solving the functional derivative from eq. 2 yields:

$$\frac{\delta F}{\delta \phi} = 2f_0 \phi (1 - \phi)^2 + 2f_0 \phi^2 (\phi - 1) - K_\phi \nabla^2 \phi \Leftrightarrow \quad (4a)$$

$$\Leftrightarrow 2\phi^3 - 4\phi^2 + 2\phi - K_\phi \nabla^2 \phi \quad (4b)$$

Inserting the result into eq. 2 results in:

$$\frac{\partial \phi}{\partial t} = -L[f_0(2\phi^3 - 4\phi^2 + 2\phi) - K_\phi \nabla^2 \phi] \quad (5)$$

As the governing equation for solving the PDE we apply Neumann boundary conditions for the left  $\phi_0 = \phi_1$  and the right side  $\phi_n = \phi_{n-1}$  and discretize the partial derivative  $\frac{\partial \phi}{\partial t}$  as:

$$\frac{\partial \phi}{\partial t} \approx \frac{\phi_{next} - \phi}{\Delta t} = -L[f_0(2\phi^3 - 4\phi^2 + 2\phi) - K_\phi \nabla^2 \phi] \Leftrightarrow \quad (6a)$$

$$\Leftrightarrow \phi_{next} = \phi - \Delta t L[f_0(2\phi^3 - 4\phi^2 + 2\phi) - K_\phi \nabla^2 \phi] \quad (6b)$$

and  $\nabla^2 \phi(x)$  is discretized according to the (central) finite differences scheme:

$$\nabla^2 \phi(x_i) \approx \frac{\phi(x_{i+1}) - 2\phi(x_i) + \phi(x_{i-1}))}{\Delta x^2} \quad (7)$$

where  $x_i$  is the node at which the value is computed and  $\Delta x$  is the node distance. The initial result is plotted in fig. 1. As can be seen in fig. 2 with decreasing  $f_0$  the total energy decreases faster over time. With decreasing value the transition region (where  $\phi$  changes from 0 to 1) becomes broader. The opposite effect can be observed in fig. 3 with variation of  $K_\phi$ . Additional the energy density functional seems to become broader but only changes its peak value for increased K-values. L does not seem to have any influence on the  $\phi$ -field, the energy or energy density - see fig. 4 .

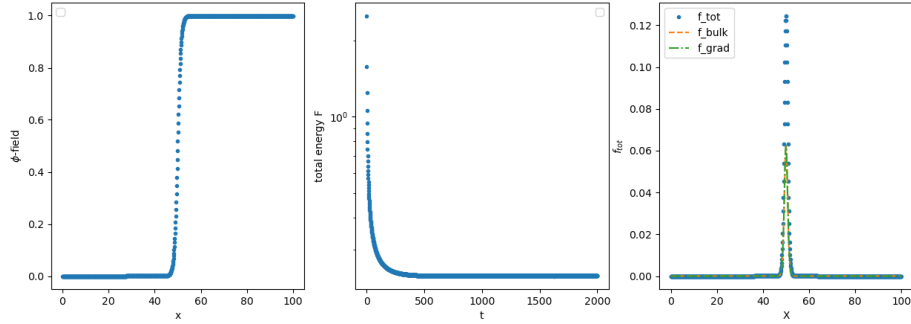


Figure 1: Initial results of the 1D single-component solidification simulation.

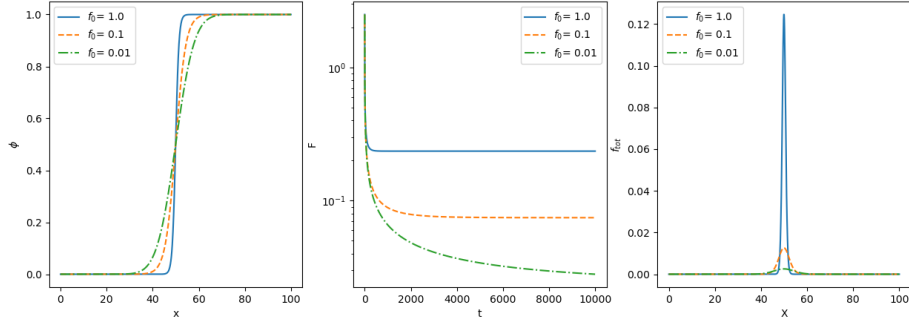


Figure 2: Results of the 1D single-component solidification simulation with various  $f_0$  values, with constant values  $K=0.1$  and  $L = 1$ .

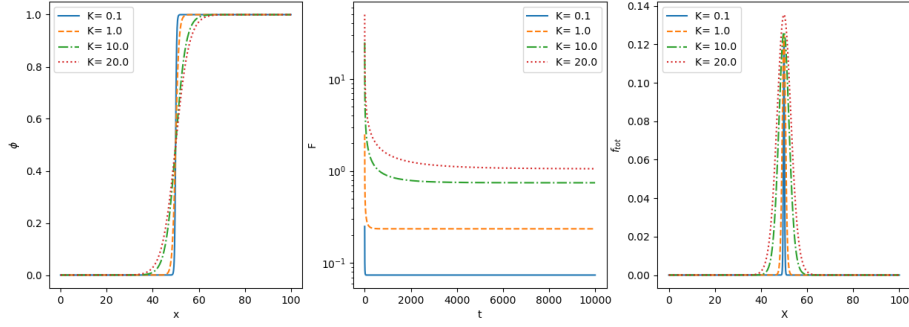


Figure 3: Results of the 1D single-component solidification simulation with various  $K$  values with constant values  $f_0 = 1$  and  $L = 1$ .

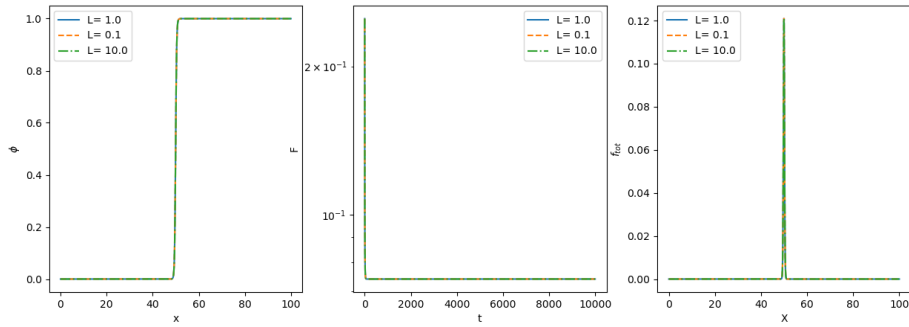


Figure 4: Results of the 1D single-component solidification simulation with various  $L$  values with constant values  $K = 0.1$  and  $f_0 = 1$ .

### 3 Task 2: Determination of $f_0$

The equilibrium Al concentration of the disordered  $\gamma$ -Phase  $c_\gamma^e$  has been determined to be 0.165 and the Al concentration of the ordered  $\gamma'$ -Phase  $c_{\gamma'}^e$  has been determined to be 0.230 - which is shown in fig. 5 [1]. This however clashes with the value that is shown in the problem statement [2] - which features the following fig. 6. For reasons of consistency we will assume  $c_\gamma^e$  to be 0.16 and  $c_{\gamma'}^e$  to be 0.23. The bulk energy density function is constructed as:

$$f_{bulk} = f_0(c_{\gamma'}^e - c)^2(c_\gamma^e - c)^2 \quad (8)$$

The  $f_0$  needs to be fitted so that it results in an energy barrier of  $\Delta f = 149 \frac{\text{J}}{\text{mol}}$  [2]. This is accomplished by choosing the right  $f_0$  to reach the right value at the local maximum of eq. 8. The local maximum of the function can be found automatically by finding the second root of the derivative of eq. 8:

$$\frac{df_{bulk}}{dc} = -2f_0(c_{\gamma'}^e - c)(c - c_\gamma^e)^2 + 2f_0(c_{\gamma'}^e - c)^2(c - c_\gamma^e) \quad (9)$$

Factoring out  $f_0(c_{\gamma'}^e - c)(c - c_\gamma^e)$  to find the root of the function we are left with:

$$c_{max} = \frac{1}{2}(c_\gamma^e + c_{\gamma'}^e) \quad (10)$$

Here  $c_{max}$  is found at 0.195. Solving 8 for  $f_0$  results in a value of  $\approx 100.9 \cdot 10^6 \frac{\text{J}}{\text{mol}}$ . The resulting function of the corresponding parameters is plotted in 7.

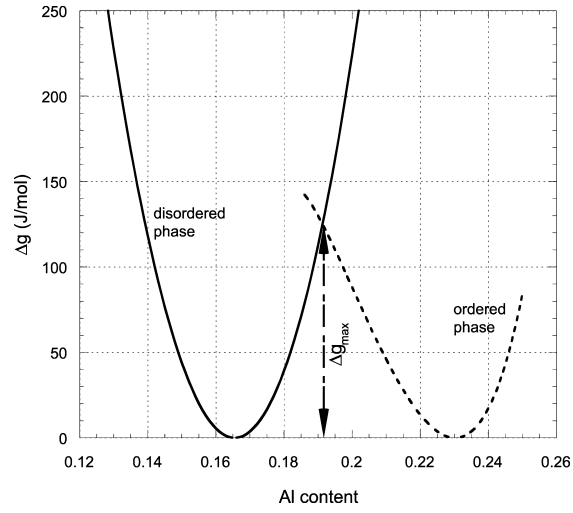


Figure 5: Calculated chemical free energy as a function of composition for both the disordered and ordered phase at 1300 K reproduced from [1].

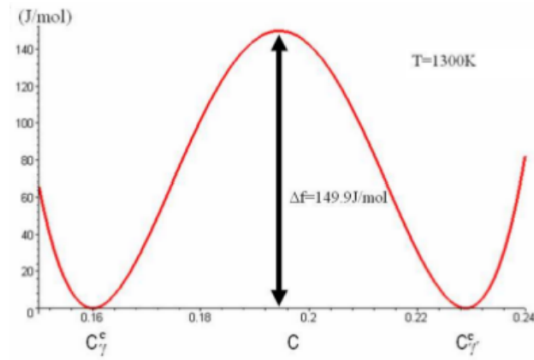


Figure 6: Bulk energy density as a function of concentration of Al at 1300 K reproduced from [2].

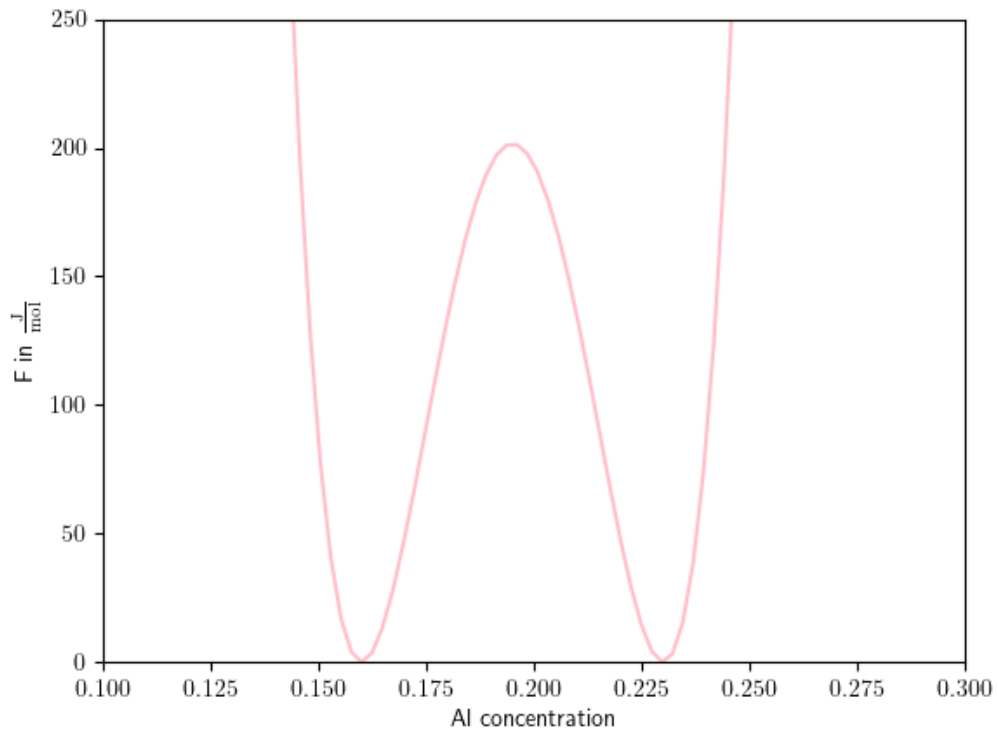


Figure 7: Plot of bulk energy of binary NiAl mixture with  $c_{\gamma}^e = 0.165$ ,  $c_{\gamma'}^e = 0.23$  and  $f_0 = 133.6 \cdot 10^6 \frac{\text{J}}{\text{mol}}$ .



## 4 Task 3: Determination of $K_c$

In this task the gradient energy density coefficient of a binary NiAl-system is calculated. Apart from the governing equation being the Cahn-Hilliard equation (eq. 11) as we are dealing with a conserved field, the general algorithm is similar to sec. 2.

$$\frac{\partial c}{\partial t} = M \nabla^2 \frac{\delta F}{\delta c} \quad (11)$$

The functional for the binary system is evaluated as follows:

$$\frac{\delta F}{\delta c} = 2f_0(c_{\gamma'} - c)(c - c_{\gamma})^2 + 2f_0(c - c_{\gamma})(c_{\gamma'} - c)^2 - K_c \nabla^2 c \quad (12)$$

$\nabla^2(\cdot)$  is (both in eq. 12 and eq. 11) is discretized as in sec. 2 eq. 7. The following coefficients are used molar Volumen  $V_m = 10^{-5} \frac{m^3}{mol}$ , interface mobility  $M = 10^{-17} \frac{mol^2}{Jms}$ , length segment  $dx = 10^{-8}m$ ,  $f_0 = 134 \cdot 10^6 \frac{J}{mol}$  and a experimental interface energy of  $F_{inte} = 5 \sim 50 \cdot 10^{-3} \frac{J}{m}$ .

As  $M$  is function of molar quantity of substance for calculating the energy we have to define an adjusted  $M_{new} = MV_m^2$ . Running the simulation for various values of  $K_c$  results in fig. 8. The total energies  $F$  are calculated, by applying the `numpy.trapz` method - integrating  $f_{inte}$  over  $x$ . Printing the energies alongside the  $K_c$  values shows that  $1.0 \cdot 10^{-6} < K_c < 1.0 \cdot 10^{-7} \frac{J}{m}$  produced results in the experimentally observed Range of  $0.05 < F_{inte} < 0.5 \frac{J}{mol}$ .

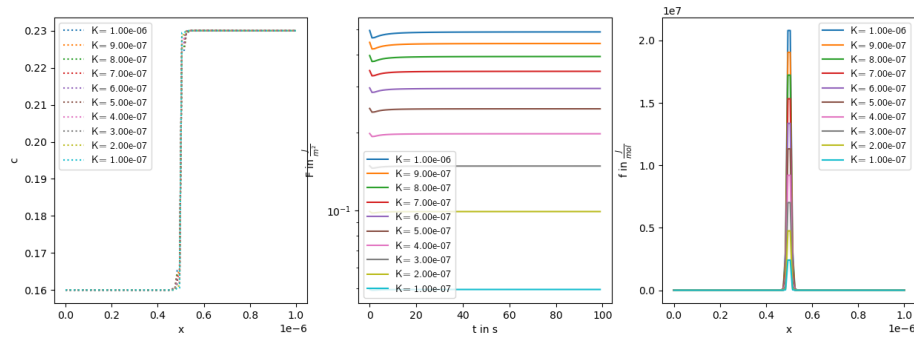


Figure 8: Results of the conserved binary NiAl-system simulation with various  $K_c$  values.

For expanding the calculation of the concentrations we need to implement eq. 7 in 2D:

$$\nabla^2 c_{i,j} = \frac{c_{i,j-1} + c_{i,j+1} - 4c_{i,j} + c_{i-1,j} + c_{i+1,j}}{\Delta x^2} \quad (13)$$

where the concentrations are mapped on a  $n \times n$ -Matrix. Running the simulation for  $1000dt$  results in fig. 10 and . Here we applied an initially random concentration with  $c_{init} = 0.195$  as a mean value for a gauss distributed matrix using the `numpy.random.normal(loc=0.195, scale=0.1, size=(N,N))` function. Choosing unfitting K values (i.e.  $3 \cdot 10^{-5}$ ) we see that the formation of domains does not occur - fig. 9. While for the K value  $1 \cdot 10^{-6}$  over time we see, the development of several domains of  $\gamma$   $\gamma'$ -Phases - fig. 10. For smaller values like  $10^{-7}$  the domains become thinner, and less pronounced 11.

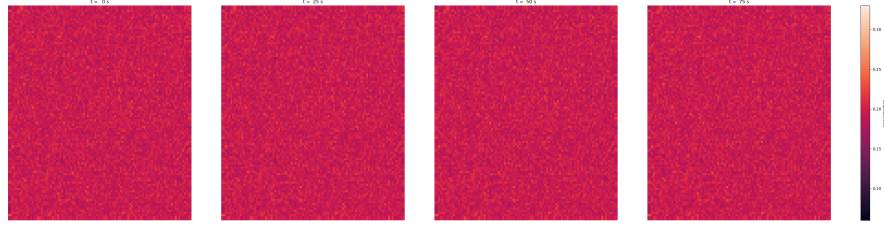


Figure 9: Heatmaps of concentrations over time calculated by conserved phase-field method from an initially randomly distributed concentration map with a K value of  $3 \cdot 10^{-5}$ .

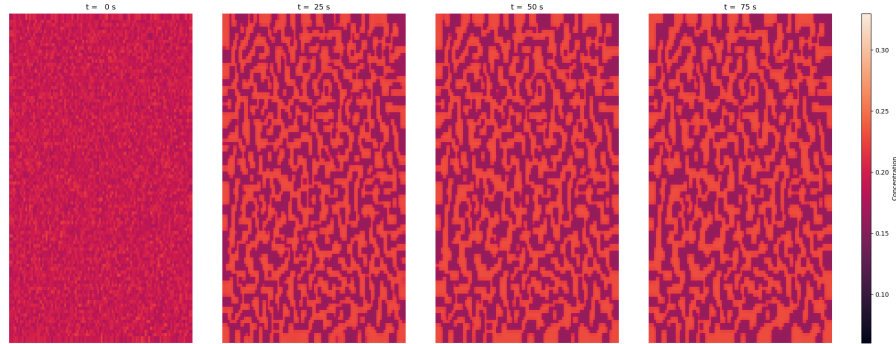


Figure 10: Heatmaps of concentrations over time calculated by conserved phase-field method from an initially randomly distributed concentration map with a  $K$  value of  $10^{-6}$ .

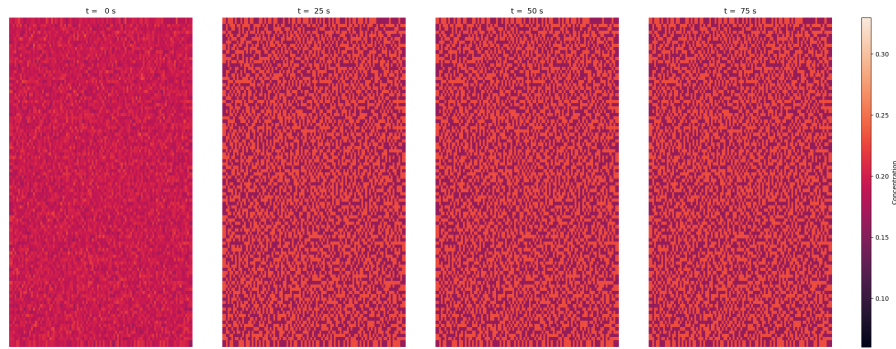


Figure 11: Heatmaps of concentrations over time calculated by conserved phase-field method from an initially randomly distributed concentration map with a  $K$  value of  $10^{-7}$ .

## References

1. Zhu, J. Z., Liu, Z. K., Vaithyanathan, V. & Chen, L. Q. Linking Phase-Field Model to CALPHAD: Application to Precipitate Shape Evolution in Ni-base Alloys. *Scripta Materialia* **46**, 401–406. ISSN: 1359-6462. <https://www.sciencedirect.com/science/article/pii/S1359646202000131> (2024) (Mar. 11, 2002).
2. Zaiser, M. *Problem Statement: Phase-field Method: Basics and Application in Materials Science*